論文 / 著書情報
Article / Book Information

Title	Increasing the ductility of ultrafine-grained copper alloy by introducing fine precipitates
Author	Naoki Takata, Yusuke Ohtake, Kazuhisa Kita, Kazuo Kitagawa, Nobuhiro Tsuji
Journal/Book name	Scripta Materialia, Vol. 60, , pp. 590-593
Issue date	2009, 4
URL	http://www.journals.elsevier.com/scripta-materialia/
DOI	http://dx.doi.org/10.1016/j.scriptamat.2008.12.018
Note	このファイルは著者（最終）版です。 This file is author (final) version.

Ductility Increase in Ultra-Fine Grained Copper Alloy by Introducing Fine Precipitates

Naoki Takata [1*], Yusuke Ohtake[2] , Kazuhisa Kita[2]
Kazuo Kitagawa[2] and Nobuhiro Tsuji [3],

[1] Dept. of Metallurgy and Ceramics Science, Tokyo Institute of Technology, 2-12-1-S8-8 Ookayama, Megro-ku, Tokyo, 152-8552, Japan

[2] Dept. of Mechanical Systems Engineering, Kanazawa University, Kakuma-machi, Kanazawa, 920-1192, Japan

[3] Dept. of Adaptive Machine Systems, Osaka University, 2-1 Yamadaoka, Suita, Osaka, 565-0871, Japan

Key words: severe plastic deformation; accumulative roll bonding; mechanical property; precipitation; Cu-Cr-Zr alloy

*Corresponding author, Tel.:+81-3-5734-2801, Fax:+81-3-5734-3585, .
E-mail address : ntakata@mtl.titech.ac.jp (N. Takata)

Abstract

In the present study, we fabricated the ultra-fine grained (UFG) Cu-Cr-Zr alloy including fine second phase particles through the accumulative roll bonding (ARB) process and subsequent aging treatment. The nano-sized precipitates dispersing within the UFG matrix significantly enhanced strain hardening, resulting in the simultaneous improvement of uniform elongation and tensile strength.

It is generally known that severe plastic deformation (SPD) of metallic materials results in ultra-fine grained (UFG) microstructure with mean grain size much smaller than 1 μm [1]. The bulky UFG materials are attractive for engineering application because they perform 3-4 times higher strength than that of the same materials with conventional grain sizes of 10-100 μm [1-5]. However, the ductility (especially, uniform elongation) is significantly limited in the UFG materials, which is the critical issue for the practical application of the UFG materials. The limited uniform elongation of the UFG materials can be simply understood in terms of early plastic instability. It is well known that the uniform elongation in tensile test is determined by plastic instability, in other word, necking condition. Considére criterion for plastic instability in rate-insensitive materials is expressed as

$$\sigma \geq \left(\frac{d\sigma}{d\varepsilon} \right) \tag{1}$$

where σ and ε are true stress and true strain, respectively, so that ($d\sigma/d\varepsilon$) is strain hardening rate. When the strain-hardening rate coincides with the flow stress, plastic instability (macroscopic necking) starts in the tensile test, which determines the uniform elongation. The limited uniform elongation in the UFG materials is attributed to high yield strength and poor strain hardening in such microstructures [5]. At the same time, however, eq.(1) represents that it is possible to increase the uniform elongation if the strain hardening rate can be increased. One of possible ways to enhance strain hardening is to introduce fine dispersoids within the UFG microstructure for accumulating an excessively large number of dislocations. In the present study, we have found that it is actually possible to manage both high strength and adequate ductility in the UFG Cu alloy by introducing fine precipitates within the UFGs.

The material used in this study is a Cu-0.85wt%Cr-0.07wt%Zr alloy. The Cu-Cr-Zr alloy is well known as a commercial precipitation hardened material. This alloy is used in some applications where high mechanical strength and electrical (or thermal) conductivity are concurrently required, such as electrodes for point welding, and heat exchangers [e.g. 6]. An ingot of the Cu-0.85wt%Cr-0.07wt%Zr alloy was firstly solution

treated at 1000℃ for 6.6 ks and quenched. The solution-treated material was cold rolled to a reduction of 80% (equivalent strain: 1.9). The cold-rolled sheet with 1 mm in thickness was used as the starting sheet for the ARB process. The principle and detailed processing procedures of the ARB process have been reported previously [2-4]. The ARB process using 50% reduction per cycle was carried out up to an equivalent strain of 4.8 (6 ARB cycles) with lubrication at room temperature. Total equivalent strain accumulated in the initial cold-rolled and ARB was therefore 6.7. The ARB processed sheet was aged at 450℃ for 2ks. This optimum aging condition for high strength has been found in the preliminary investigation for the ARB specimen aged at various temperatures [7]. The microstructural characterization of the specimens was carried out by electron backscattering diffraction pattern (EBSD) measurement in a field emission type scanning electron microscope (FE-SEM) and by transmission electron microscopy (TEM). For EBSD measurement, the sections perpendicular to transverse direction (TD) of the sheet were mechanically polished with sandpapers and then electro-polished in a solution of phosphoric acid and water of 3: 7 in volume. The EBSD measurements were carried out by the use of FE-SEM (FEI Philips XL30) equipped with TSL-OIM (Orientation Imaging Microscopy) system at an accelerate voltage of 15 kV. The step size used in the EBSD measurements was 0.05 μm. For TEM observations, thin specimens perpendicular to TD of the sheet were mechanically polished to approximately 50 μm in thickness and then electro-polished in the same solution as that for the EBSD specimen. The TEM observations were carried out with Hitachi H-800 operated at 200 kV. The tensile test of each specimen was carried out at an initial strain rate of 1.0×10^{-3} s^{-1} at room temperature.

Figure 1 shows grain boundary maps obtained from the EBSD measurement of the as cold-rolled (0-cycle ARB) and 6-cycle ARB processed Cu-Cr-Zr alloy specimens. These images were obtained at the quarter thickness location on the longitudinal section of the ARB processed sheets. In the figures, green lines indicate high angle boundaries whose misorientation is larger than 15 degrees, while red lines low angle boundaries with misorientation ranging from 2 degrees to 15 degrees. The boundaries having misorientation smaller than 2 degrees were cut off, in order to remove the

inaccuracy in EBSD measurement and analysis. The microstructural parameters obtained from the EBSD measurements were summarized in Table 1. The EBSD measurement revealed that significant grain refinement was achieved by 6-cycle ARB. The 0-cycle specimen (80% cold-rolled) showed a typical deformation microstructure where initial grains involving substructures were elongated to the rolling direction (RD). After 6-cycle ARB, the ultra-fine lamellar boundary structure including high density of high angle boundaries was found in Fig.1(b). The mean spacing of the high angle boundaries along ND was 0.24 μm and the fraction of high angle boundaries was 64%. The morphology of the microstructure observed in the Cu-Cr-Zr alloy severely deformed by the ARB was quite similar to those of the ARB processed pure Cu and Cu alloys previously reported [8,9].

Figure 2 shows TEM microstructures of the 6-cycle ARB processed specimen (a) and that subsequently aged at 450℃ for 2 ks (b),(c). In the 6-cycle ARB specimen (Fig.2(a)), the ultra-fine lamellar boundary structure corresponding to Fig.1(a) was observed. There are dislocations of high density within the ultra-fine lamellas. The ultra-fine lamellar structure was maintained even after aging at 450℃ for 2ks, as shown in Fig.2(b). The fraction of high angle boundary and mean spacing of high angle boundaries in the aged specimen, which were checked by EBSD measurement, were almost the same as those of the as-ARB processed specimen (Table 1). While the dislocation substructure scarcely changed after the aging, fine precipitates appeared in the UFG microstructure of the aged specimen, as shown in Fig.2 (c). It should be emphasized that the nano-sized precipitates whose size is less than 10 nm distributed within the ultra-fine lamellar grains as well as on grain boundaries. In our previous study on the ARB processed and aged Al-2wt%Cu alloy, the precipitates are predominantly localized at grain boundaries of the UFG microstructure and coarsened much faster than those in the coarse grained materials [10]. The present precipitation behavior is fairly different from that reported in the Al-Cu system [10], though the precipitation on grain boundaries is also recognized. Such an in-grain precipitation in the UFG microstructure fabricated by SPD processes has been reported in a few papers [11-13]. For example, Horita et al. [13] have reported precipitation of fine Ag particles

within UFGs in an ECAP (equal channel angular pressing) processed Al-Ag alloy. However, the Al-Ag system has a large solubility of Ag and they used an alloy with high concentration of Ag (Al-10.8wt%Ag). It should be noted that the Cu-Cr-Zr alloy used in this study do not have high concentration of alloying elements (0.85wt%Cr-0.07wt%Zr). It has been known that in ternary Cu-Cr-Zr alloy, the precipitation of Cu_3Zr intermetallic compound occurs at about 450 °C [14,15]. Although the precipitates observed in the present study have not been identified, the stable fine precipitates within the ultra-fine lamellar grains in present Cu-Cr-Zr alloy are considered as Cu_3Zr particles. It has been also reported that Zr containing particles were finely dispersed in the UFG Cu matrix of the Cu-Zr alloy [16] and the Cu-Cr-Zr alloy [17] ECAP processed and subsequently heat treated. It can be therefore considered that the addition of trace Zr element results in the stable Zr containing particles within the UFG Cu matrix. The stability for fine precipitates is presumably attributed to low diffusivity of Zr atoms in Cu matrix.

Figure 3 shows nominal stress-strain curves of the Cu-Cr-Zr specimens at various stages of the treatments. The mechanical properties obtained from the stress-strain curves are summarized in Table 2. The 6-cycle ARB processed specimen performed higher strength than that of the 0-cycle specimen (80% cold-rolled). This result clearly shows that the evolution of the UFG microstructure by ultrahigh straining results in the significant strengthening. It is interesting that the total elongation of the 6-cycle ARB specimen is larger than that of the 0-cycle specimen. However, the uniform elongation of the 6-cycle ARB specimen is only 1.9% that is typical for SPD/UFG materials [5], though the macroscopic necking after the peak stress is not so significant compared with the 0-cycle specimen. The aged ARB specimen exhibited both higher strength and larger elongation than those of the as-ARB processed specimen. It should be emphasized that the improvement of ductility is owing to an increase in the uniform elongation, as shown in Table 2. This ductility increase is quite different from those previously reported in SPD/UFG materials where ductility is improved by a significant loss of their strength in annealing [5]. It can be considered that the fine precipitates within the UFGs of the Cu-Cr-Zr alloy play a significant role for the increase in both

strength and ductility.

In order to understand the concurrent improvement of strength and ductility, mechanical property of the materials is discussed in terms of the plastic instability based on Eq.(1). Figure 4 shows the true stress-true strain curves and strain hardening rate - true strain curves obtained from the results of the tensile test for each specimens. The point at which two curves meet agrees well with the uniform elongation measured from the nominal stress-strain curves in each specimen (Table 2), which indicates that Considére criterion (eq.(1)) stands for the present materials. Figure 4 represents that the aged ARB specimen exhibits higher strain-hardening rate than that of the as-ARB processed specimen, especially at later stage of tensile deformation. This obviously indicates that the strain hardening is enhanced by homogenously dispersed nano-precipitates within the UFG matrix introduced by aging. It can be considered that the precipitates can act as obstacles for dislocation motion although precipitate on grain boundary cannot play a role of barrier for dislocations. High density dislocations accumulated within the UFGs provide a significant strain hardening, resulting in large uniform elongation accompanied with high tensile strength. It can be therefore concluded that enhancing strain-hardening by dispersing fine second-phase particles is effective to prevent the occurrence of early plastic instability to realize adequate tensile ductility without a loss of strength in the UFG Cu-Cr-Zr alloy. Such an approach would be applicable to other alloy systems as well.

The authors would like to thank the financial support by the Grant-in-Aid for Scientific Research on the Priority Area “Giant Straining Process for Advanced Materials Containing Ultra-High Density Lattice Defects,” both through the Ministry of Education, Culture, Sports, Science and Technology (MEXT), Japan.

[1] SEVERE PLASTIC DEFORMATION, Towards Bulk Production of Nanostructured Materials, edited by B. S. Altan, I. Miskioglu, G. Purcek, R. R. Mulyukov and R. Artan, NOVA Science Publishers, New York, 2006.

[2] N. Tsuji, Y. Saito, S.H. Lee, Y. Minamino, Adv. Eng. Mater. 5(2003) 338.

[3] Y. Saito, N. Tsuji, H. Utsunomiya, T. Sakai, H.G. Hong, Scripta Mater. 39(1998)1221.

[4] Y. Saito, H. Utsunomiya, N. Tsuji, T. Sakai, Acta Mater. 47(1999) 579.

[5] N. Tsuji, Y. Ito, Y. Saito and Y. Minamino, Scripta Mater. 47(2002) 893.

[6] A.A.F. Tavassoli; J. Nucl Mater., A85(1998), 258.

[7] Y. Ootake, K. Kitagawa, K. Kita, N. Takata, N. Tsuji and S. Aoki: Journal of the JRICu 46(2007), 142.

[8] N. Takata, K. Yamada, K. Ikeda, F. Yoshida, H. Nakashima and N. Tsuji: Mater. Trans. 48(2007), 2043.

[9] N. Takata, S.-H.Lee, C.-Y. Lim, S.-S. Kim and N. Tsuji: Journal of Nanoscience and Nanotechnology 7(2007), 3985.

[10] N. Tsuji, T. Iwata, M. Sato, S. Fujimoto and Y. Minamino: Sci. Tech. Adv. Mater., 5 (2004), 173.

[11] N. Tsuji, R. Ueji, Y. Minamino and Y. Saito: Scripta Mater. 46(2002), 305.

[12] R. Ueji, N. Tsuji, Y. Minamino and Y. Koizumi: Acta Mater. 50(2002), 4177.

[13] Z. Horita, K. Ohashi, T. Fujita, K. Kaneko and T.G. Langdon: Adv. Mater. 17(2005), 1599.

[14] H. Suzuki, M. Kanno and I Kawakatsu: J. Japan Inst. Met., 33(1969), 628.

[15] H. Suzuki and M. Kanno: J. Japan Inst. Met., 36(1972), 363.

[16] Y. Amouyal, S.V. Divinski, Y. Estrin and E. Rabkin: Acta Mater. 55(2007), 5968-5979.

[17] A. Vinogradov, V. Patlan, Y. Suzuki, K. Kitagawa and V.I. Kopylov: Acta Mater. 50(2002), 1639-1651.

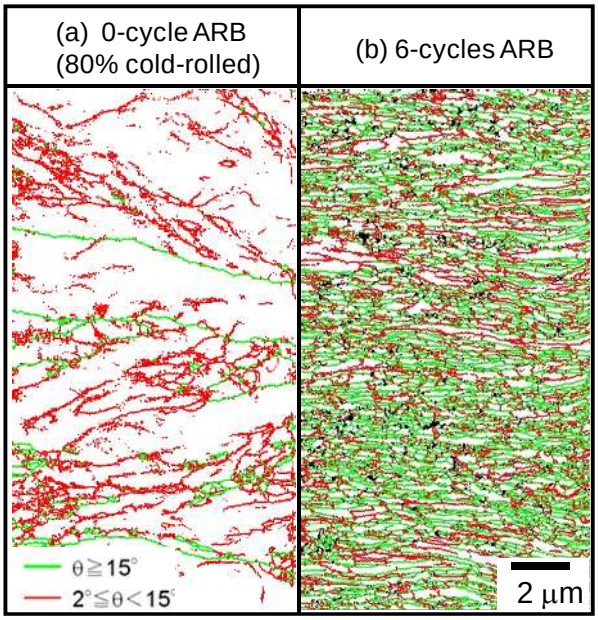

Fig.1 Boundary maps of 80% cold rolled Cu-Cr-Zr alloy (0-cycle ARB) (a), Cu-Cr-Zr ARB processed by 6 cycles (b). In boundary maps, red lines represent the misorientation (q) of $2^\circ \leq \theta < 15^\circ$, while green lines represent $15^\circ \leq \theta$.

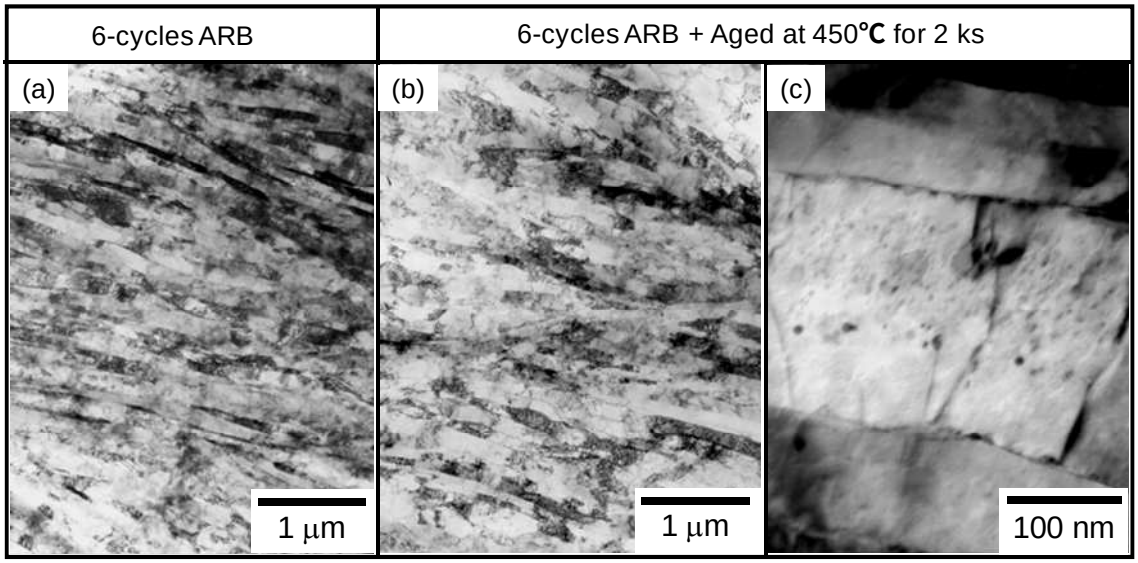

Fig.2 TEM microstructures of the ARB processed Cu-Cr-Zr alloy (a) and the Cu-Cr-Zr alloy 6-cycle ARB processed and aged at 450℃ for 2 ks (b)(c).

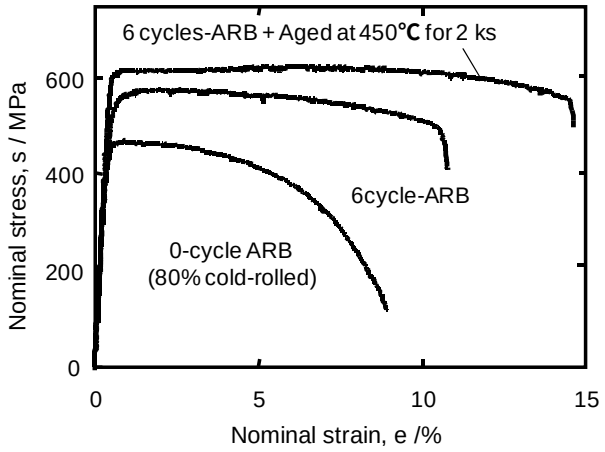

Fig.3 Nominal stress-strain curves of the 80% cold-rolled Cu-Cr-Zr alloy (0-cycle ARB), the ARB processed Cu-Cr-Zr alloy and the Cu-Cr-Zr alloy ARB processed by 6 cycles and subsequently aged at 450℃ for 2 ks.

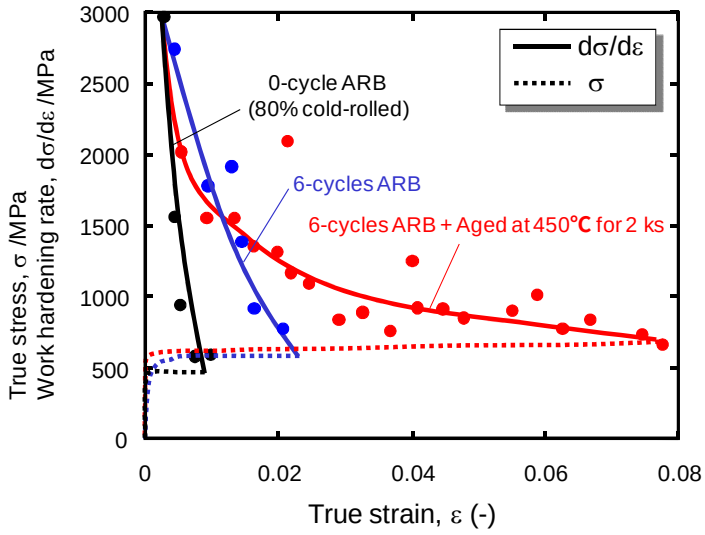

Fig.4 True stress-true strain curves and work hardening rate-true strain of the 80% cold-rolled Cu-Cr-Zr alloy (0-cycle ARB), the ARB processed Cu-Cr-Zr alloy and the Cu-Cr-Zr alloy ARB processed and subsequent aged at 450℃ for 2 ks.

Table1 Microstructural parameters obtained from EBSD measurement of the specimens.

	Mean spacing of high angle boundaries along ND (μm)	Grain Aspect ratio	Fraction of high angle boundaries (%)
0-cycle ARB (as-80% cold rolled)	4.3	-	20.6
6-cycle ARB	0.23	4.1	63.1
6-cycle ARB + Aged at 450℃ for 2 ks	0.26	4.0	67.4

Table2 Mechanical properties of the specimens.

	0.2% proof strength (MPa)	Tensile strength (MPa)	Uniform elongation (%)	Total elongation (%)
0-cycle ARB (as-80% cold rolled)	459	464	0.6	8.7
6-cycle ARB	542	573	1.9	10.5
6-cycle ARB + Aged at 450℃ for 2 ks	608	625	7.6	14.3